

# AN UPGRADED LHC INJECTION KICKER MAGNET\*

M. J. Barnes<sup>†</sup>, C. Bracco, G. Bregliozzi, A. Chmielinska, L. Ducimetière, B. Goddard, T. Kramer, H. Neupert, L. Vega Cid, V. Vlachodimitropoulos, W. Weterings, C. Yin Vallgren, CERN, Geneva, Switzerland

## Abstract

An upgrade of the LHC injection kickers is necessary for HL-LHC to avoid excessive beam induced heating of these magnets: the intensity of the HL-LHC beam will be twice that of LHC. In addition, in the event that it is necessary to exchange an injection kicker magnet, the newly installed kicker magnet would limit HL-LHC operation for a few hundred hours due to dynamic vacuum activity. Extensive studies have been carried out to identify practical solutions to these problems: these include redistributing a significant portion of the beam induced power deposition to ferrite parts of the kicker magnet which are not at pulsed high voltage and water cooling of these parts. Furthermore a surface coating, to mitigate dynamic vacuum activity, has been selected. The results of these studies, except for water cooling, have been implemented on an upgraded LHC injection kicker magnet: this magnet was installed in the LHC during the 2017-18 Year End Technical Stop. This paper presents the upgrades, including some test and measurement results.

## INTRODUCTION

The Large Hadron Collider (LHC) is equipped with two injection kicker (MKI) systems, MKI2 and MKI8, for deflecting the incoming particle beams onto the LHC's equilibrium orbits [1]. Counter-rotating beams circulate in two horizontally separated pipes. Each beam pipe is filled by 12 consecutive injections, at 450 GeV. Both MKI2 and MKI8 comprise four systems, named A through D: D is the first to see injected beam. The total deflection by an MKI system is 0.85 mrad, requiring an integrated field strength of 1.3 T·m. To limit beam emittance blow-up due to injection oscillations, reflections and flat top ripple of the field pulse must be less than  $\pm 0.5\%$ .

A low impedance ( $5 \Omega$ ) and carefully matched high bandwidth system meets the stringent pulse response requirements. An MKI kicker system consists of a multi-cell Pulse Forming Network (PFN) and a multi-cell travelling wave kicker magnet [2], connected by a matched transmission line and terminated by a matched resistor (TMR). Each travelling wave magnet has 33 cells. A cell consists of a U-core NiZn ferrite sandwiched between high voltage (HV) plates: ceramic capacitors are sandwiched between each HV plate and a plate connected to ground (Fig. 1). The magnets are operated in vacuum of  $\sim 10^{-11}$  mbar. The complete magnet is baked out at  $315^\circ\text{C}$  before HV conditioning and tests.

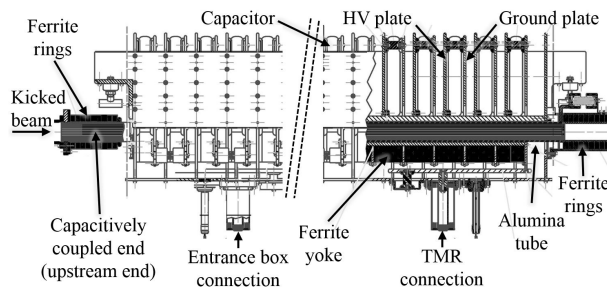


Figure 1: MKI kicker magnet.

## BEAM INDUCED HEATING

With high bunch intensity and short bunch lengths, integrated over many hours of a good physics fill, the impedance of the magnet ferrite yoke can lead to significant beam induced heating. To limit longitudinal beam coupling impedance, while allowing a fast magnetic field rise-time, an alumina tube with screen conductors lodged in its inner wall is placed within the aperture of the magnet [2]. The conductors, which provide a path for the image current of the beam, are connected to the standard LHC vacuum chamber at one end and are capacitively coupled to it at the other end. There is a set of toroidal ferrite rings mounted around each end of the alumina tube, outside of the aperture of the magnet (Fig. 1), whose original purpose was to damp low-frequency resonances [3]. Each set of nine toroids, historically, utilizes two types of NiZn ferrite [4].

High temperatures in the ferrite yokes of the MKIs can also potentially limit the performance of the LHC. Once the yokes exceed their Curie temperature ( $T_c$ ), their magnetic permeability is, temporarily, significantly decreased [5], which would lead to mis-injecting beam: this may damage neighbouring equipment.

### Temperatures in 2017

To monitor the temperatures, two thermal probes (PT100s) are installed per end of each of the eight kicker magnets. The upstream end probes consistently measure higher temperatures than the downstream ones and therefore are of primary concern. Since the ferrite yokes are pulsed at high voltage (HV) during operation, the probes are placed at neighbouring locations at ground potential, thus providing only indirect temperature measurements.

The power deposition, and hence temperature distribution, is highly non-linear in the ferrite yoke [6–10]. Power deposition derived from detailed CST [11] simulations has been used as input to transient and steady-state thermal simulations: there is good agreement between measured and

\* Work supported by the HL-LHC project.

<sup>†</sup> mike.barnes@cern.ch

Content from this work may be used under the terms of the CC BY 3.0 licence (© 2018). Any distribution of this work must maintain attribution to the author(s), title of the work, publisher, and DOI.

predicted side-plate temperatures [9], validating the power loss calculations and the thermal model.

Due to the criticality of the yoke temperatures on the performance of the MKI, and thus on the safety of the injection, an injection interlock is activated when measured temperatures exceed pre-set SIS (Software Interlock System) thresholds: these thresholds are defined separately for each of the PT100s associated with the ferrites yokes.

A SoftStart, i.e. pulsing the kicker magnets without beam present, is run following a beam dump: after each SoftStart there is a careful analysis of measured waveform parameters (magnet delay and rise time of its output pulse): using this procedure it is possible to ensure that the ferrite yokes are below their Curie temperature [12]. If an SIS threshold has been exceeded, and the analysis shows that the ferrite yoke is below its Curie point, the appropriate SIS threshold is increased by  $1^{\circ}\text{C}$  above the measured temperature. An increase of  $1^{\circ}\text{C}$  is chosen as, if the first ferrite yoke reaches  $T_c$ , as a result of the non-linear power deposition the second yoke is expected to be almost  $10^{\circ}\text{C}$  lower (see Fig. 1 of ref. [10]): thus only one yoke (3.3% of a magnet, 0.8% of a kicker system) would exceed the  $T_c$ . During 2017 the downloading and plotting of measured waveform parameters was automated, speeding up this analysis procedure.

### *Future Plans for Beam Induced Heating*

For Run 3 operation, with High Luminosity (HL) LHC type beams, the power deposition in the MKIs is expected to be a factor of  $\sim 4$  greater than for LHC: this would be unacceptably high unless measures are taken. Hence means of reducing heating of the yoke [8] and efficiently removing heat from the magnet [9] are being studied. The ferrite yokes cannot be directly cooled as they are at pulsed HV. One very promising approach is to relocate the power deposition to the upstream ferrite rings, rather than the upstream yokes [6, 7]: the upstream ferrite rings can then be cooled [10]. Relocating power deposition is achieved by increasing exposure of the upstream ferrite rings to electromagnetic power radiated from the "open" ends of the beam screen conductors [6].

An upgraded MKI kicker magnet was installed in the LHC during the Year End Technical Stop (YETS) 2017-18. The primary purpose of the installation is to validate, with beam,  $\text{Cr}_2\text{O}_3$  applied to the inner surface of the alumina tube (see below). The opportunity was also taken to redistribute power deposition from the yoke to the upstream ferrite rings: the predicted temperature of the ferrite rings is significantly increased [6]. Hence measured ring temperatures will be used to validate the predicted redistribution. Simulations of the vacuum system show that the higher ring temperature does not significantly increase the predicted vacuum pressure in this region. Despite the lower power deposition in the yokes the maximum yoke temperature is not greatly influenced because of increased heat conduction from the ferrite rings, along the alumina tube, to the yokes.

## HV PERFORMANCE

The original beam screen installed in each kicker magnet was designed to have 24 screen conductors. However, as a result of problems with electrical flashover on the inner surface of the alumina tube, when the kicker magnet was pulsed, only 15 screen conductors could be installed [13]. Nevertheless, as a result of excessive heating of an MKI magnet, it was necessary to further reduce the real component of beam coupling impedance, by installing additional screen conductors [14]. Hence it was also necessary to reduce the flashover rate on the surface of the alumina: Ref. [15] shows that a  $\text{Cr}_2\text{O}_3$  coating on alumina gives a  $\sim 30\%$  increase in voltage of flashover in vacuum, in comparison with uncoated alumina. A more recent publication [16] also reports a  $\sim 30\%$  increase in voltage of flashover, which was attributed to the following characteristics of the chromium oxide coating:

- reducing secondary electron avalanche;
- reducing surface charging due to decreased surface resistance ( $10^{10} - 10^{11} \Omega\text{-cm}$ ).

Thus a series of studies were launched to identify the best means of coating the inside of a 3 m long alumina tube with  $\text{Cr}_2\text{O}_3$  [17]. In addition, since the  $\text{Cr}_2\text{O}_3$  decreases the SEY of the surface it could be beneficial for reducing dynamic vacuum due to electron cloud.

## ELECTRON CLOUD

Significant pressure rise, due to electron cloud, occurs in and nearby the MKIs: the predominant gas desorbed from surfaces is  $\text{H}_2$ . Conditioning of surfaces reduces electron cloud, and thus dynamic pressure rise, but further conditioning is often required when beam parameters (e.g. bunch spacing, length and intensity) are pushed. Voltage is induced on the screen conductors during field rise (to 30 kV) and fall (to  $-17$  kV). High pressure, at the capacitively coupled end, can result in breakdown/flashover: hence a SIS interlock prevents injection when the pressure is above threshold. The SIS thresholds, for the MKI interconnects, are  $5 \times 10^{-8}$  mbar. During mid-2016 electron cloud resulted in a factor of  $\sim 20$  rise in pressure in most MKI8 interconnects: the dynamic pressure rise in the MKI tanks was a factor of  $\sim 10$  [18].

Several methods have been tested for reducing the SEY of alumina. The most promising is to apply a coating of  $\text{Cr}_2\text{O}_3$ , to the inside of the alumina tube, by magnetron sputtering. Measurements show that naked, high-purity, alumina has a maximum SEY ( $\delta_{max}$ ) of 9. Measurements also show that  $\text{Cr}_2\text{O}_3$  coating, applied by magnetron sputtering, reduces  $\delta_{max}$  to 2.3 or less: bombarding the surface with electrons further reduces  $\delta_{max}$  to less than 1.4 [18].

Outgassing measurements of  $\text{Cr}_2\text{O}_3$  coated alumina plates were carried out by the CERN vacuum group: at  $20^{\circ}\text{C}$  outgassing is close to that of the sample chamber alone, so it is hard to distinguish a difference. Outgassing is only slightly higher than the chamber at  $200^{\circ}\text{C}$ . Hence the  $\text{Cr}_2\text{O}_3$  coating, applied by magnetron sputtering, is vacuum compatible.

A set of aluminium plates has been sputtered with 50 nm of  $\text{Cr}_2\text{O}_3$  and installed in a setup in the CERN Super Proton

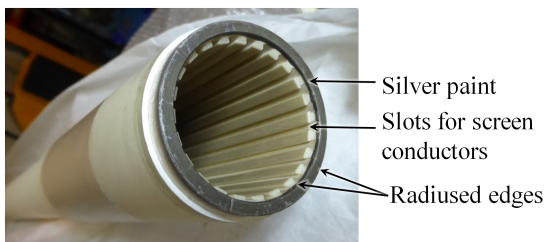


Figure 2: Photograph of one end of the alumina tube, with silver paste and  $\text{Cr}_2\text{O}_3$  coating by magnetron sputtering.

Synchrotron (SPS), during the Extended YETS 2016-17, for tests with beam: the test setup included electron cloud monitors. Unfortunately some of the wires associated with these monitors were damaged, so that not all the channels were available for read-back. Although the setup does not allow one to measure a value for the SEY of the samples under test, conditioning of the  $\text{Cr}_2\text{O}_3$  with beam was clearly visible. Hence the inner surface of a 3 m long alumina tube was coated with  $\text{Cr}_2\text{O}_3$ , by Polyteknik [19], for installation in the upgraded MKI. In order to ensure that the  $\text{Cr}_2\text{O}_3$  potential is well defined, it is connected to local ground at each end of the alumina tube. This is achieved by radiusing the ends of the alumina tube and then using C 1075 D Conductor Paste, from Heraeus [20], which extends a few mm into the inside of the alumina tube (Fig. 2): the silver paste, on the outside at each end of the tube, is connected to local ground.

The paste is cured by baking to  $850^\circ\text{C}$  in air. Measurements show that heating to  $300^\circ\text{C}$  in vacuum has only a small effect on the SEY of the  $\text{Cr}_2\text{O}_3$ : hence the magnet bakeouts should not significantly influence the SEY of the coating. However, following heating to  $850^\circ\text{C}$  the SEY is increased (Fig. 3): in addition, even after conditioning the  $\delta_{max}$  ( $\sim 1.9$ ) isn't as low as the "as received" sample or the sample heated to only  $300^\circ\text{C}$ . Hence the  $\text{Cr}_2\text{O}_3$  is only applied to the alumina tube after the silver paste has been applied and cured. Two alumina witness samples were coated together with the alumina tube, at Polyteknik. The measured  $\delta_{max}$  of the witness samples was in the range 1.3 to 1.5: bombarding the surface with electrons had little influence upon the measured  $\delta_{max}$ .

## HV TESTS ON THE UPGRADED MKI

Once the MKI magnets are assembled and aligned in their vacuum tanks, in a clean room, the complete magnet and tank are baked to  $315^\circ\text{C}$ . The oven is heated at a rate of  $5^\circ\text{C}/\text{hr}$ , held at  $315^\circ\text{C}$  for at least 72 hours, and then ramped down again at  $5^\circ\text{C}/\text{hr}$ . Afterwards the magnet undergoes a HV conditioning [2] to a pulsed voltage approximately 10% above its operational voltage. Subsequently, vacuum valves are installed, the magnet is re-baked using jackets, and then a final HV pulse conditioning is carried out. During the HV conditioning process, transparent vacuum windows were used so that the ends of the alumina tube can be observed. There was no visible corona on the surface of the  $\text{Cr}_2\text{O}_3$  coated alumina tube: corona had previously been observed on uncoated alumina. In addition, during the HV condi-

tioning processes, there weren't any flashovers that could be attributed to the surface of the  $\text{Cr}_2\text{O}_3$  coated alumina tube.

## UFOS

Pre-LS1 Unidentified Falling Objects (UFOS) occurred all around the LHC, however many events were around the MKIs [21, 22]. Extensive studies identified MKI UFOS as most likely being macro particles, of up to  $100\ \mu\text{m}$  size, which originated from the alumina tube when the screen conductors are installed in the slots [22]. Alumina tubes of all MKIs upgraded during LS1 underwent extensive cleaning processes. A final "dust-count" and analysis by scanning electron microscopy, from each alumina tube, was carried out before installing an alumina tube in an MKI; post-LS1, the MKIs no longer show up on the UFO statistics. The final dust estimate for the 8 MKIs installed during LS1 was in the range  $1.9 \times 10^6$  to  $20 \times 10^6$  particles. Similar cleaning and dust-count processes were carried out for the  $\text{Cr}_2\text{O}_3$  coated alumina tube: the final dust estimate was approximately  $1.8 \times 10^6$  particles - hence the lowest to date.

## CONCLUSION

An upgraded MKI kicker magnet has been installed in the LHC during the YETS 2017/18. The primary goal of the upgrades was to validate the  $\text{Cr}_2\text{O}_3$  coating, applied by magnetron sputtering to the inside of the alumina tube, with beam. With the  $\text{Cr}_2\text{O}_3$  coating no corona was observed in the alumina tube during HV conditioning, and no flashovers were attributed to the  $\text{Cr}_2\text{O}_3$  coated alumina tube. Furthermore, the  $\text{Cr}_2\text{O}_3$  coating is expected to significantly reduce dynamic vacuum rise due to electron cloud. The opportunity was also taken to relocate losses from the ferrite yoke to the ferrite rings, such that beam coupling impedance simulations and thermal simulations can be validated with beam. In the future a cooling system will be installed for the upstream ferrite rings, which will maintain the yoke and rings below their Curie temperatures.

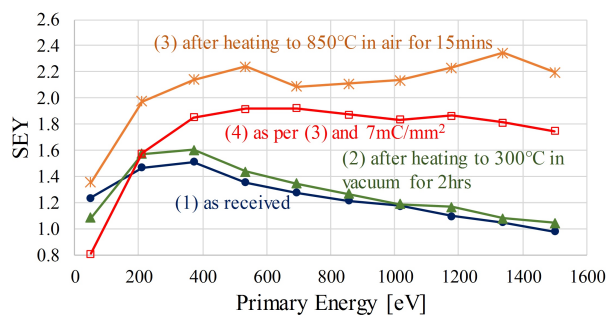


Figure 3: Measurement of SEY of 50 nm coating of  $\text{Cr}_2\text{O}_3$  on alumina: (1) as received; (2) after heating in vacuum for 2 hrs at  $300^\circ\text{C}$ ; (3) after heating in air for 15 mins at  $850^\circ\text{C}$ ; (4) as per (3) but following bombardment (conditioning) with an electron dose of  $7\ \text{mC}/\text{mm}^2$ .

## ACKNOWLEDGEMENT

The authors thank E. Garcia-Tabares Valdivieso, F. Leaux and J.A. Li Hellstrom for measurements whose results are reported in this paper. In addition, the authors thank G. Bellotto, S. Bouleghlimat, P. Burkel, P. Goll, and Y. Sillanoli for carefully preparing the upgraded MKI.

## REFERENCES

- [1] LHC design report, <http://ab-div.web.cern.ch/ab-div/Publications/LHC-DesignReport.html>
- [2] M.J. Barnes *et al.*, "Reduction of surface flashover of the beam screen of the LHC injection kickers", in *Proc. IPAC'13*, Shanghai, China, May 2013, paper MOPWA032, pp. 735-737.
- [3] H. Day *et al.*, "Evaluation of the beam coupling impedance of new beam screen designs for the LHC injection kicker magnets", in *Proc. IPAC'13*, Shanghai, China, May 2013, paper TUPME033, pp. 1649-1651. <http://www.JACoW.org>
- [4] M.J. Barnes *et al.*, "Beam induced ferrite heating of the LHC injection kickers and proposals for improved cooling", in *Proc. IPAC'13*, Shanghai, China, May 2013, MOPWA031, pp. 732-734. <http://www.JACoW.org>
- [5] A. Chmielinska, M.J. Barnes, F. Caspers, B. Kosta Popovic, C. Vollinger, "Measurements of electromagnetic properties of ferrites as a function of frequency and temperature", presented at IPAC'18, Vancouver, Canada, May 2018, paper WEPMF089, this conference. <http://www.JACoW.org>
- [6] V. Vlachodimitropoulos, M.J. Barnes, L. Vega Cid, W. Weterings, "Longitudinal impedance analysis of the upgraded LHC injection kicker magnet", presented at IPAC'18, Vancouver, Canada, May 2018, paper WEPMK002, this conference. <http://www.JACoW.org>
- [7] V. Vlachodimitropoulos, M.J. Barnes, A. Chmielinska, "Design of the beam impedance screen for the FCC-hh injection kicker magnet", presented at IPAC'18, Vancouver, Canada, May 2018, paper WEPMK004, this conference. <http://www.JACoW.org>
- [8] V. Vlachodimitropoulos, M.J. Barnes, L. Ducimetière, L. Vega Cid, W. Weterings, "Study of an improved beam screen design for the LHC injection kicker magnet for HL-LHC", in *Proc. IPAC'17*, Copenhagen, Denmark, May 2017, paper WEPVA094, pp. 3471-3474. <http://www.JACoW.org>
- [9] L. Vega Cid, M.J. Barnes, A. Abánades, V. Vlachodimitropoulos, W. Weterings, "Thermal analysis of the LHC injection kicker magnets", *J. Phys. Conf. Ser.*, 874 (2017) 012100. <https://doi.org/10.1088/1742-6596/874/1/012100>
- [10] L. Vega Cid, M.J. Barnes, V. Vlachodimitropoulos, W. Weterings, A. Abánades, "Design and test of a cooling system for the LHC injection kicker magnets", presented at IPAC'18, Vancouver, Canada, May 2018, paper WEPMK001. <http://www.JACoW.org>
- [11] CST - Computer Simulation Technology, <http://www.cst.com>
- [12] M.J. Barnes, L. Ducimetière, N. Garrel, B. Goddard, V. Mertens, W. Weterings, "Analysis of ferrite heating of the LHC injection kickers and proposals for future reduction of temperature", in *Proc. IPAC'12*, New Orleans, USA, May 21-26 2012, paper TUPPR090, pp. 2038-2040. <http://www.JACoW.org>
- [13] M.J. Barnes, F. Caspers, L. Ducimetière, N. Garrel, T. Kroyer, "An improved beam screen for the LHC injection kickers", in *Proc. PAC'07*, Albuquerque, USA, June 25-29 2007, paper TUPAN086, pp. 1574-1576. <http://www.JACoW.org>
- [14] H. Day, "Beam coupling impedance reduction techniques of CERN kickers and collimators", Ph.D. thesis, School of Physics and Astronomy, The University of Manchester, Manchester, United Kingdom, 2013, CERN-THESIS-2013-083 (available on-line).
- [15] T.S. Sudarshan and J.D. Cross, "The effect of chromium oxide coatings on surface flashover of alumina spacers in vacuum", *IEEE Trans. Electr. Insul.*, EI-11 (1976) 32. DOI: 10.1109/TEI.1976.297942
- [16] T. Shioiri, N. Asari, S. Saito, H. Nakamuta, M. Homma, K. Suzuki, "Effect of chromium oxide coating on surface flashover characteristics of ceramic in vacuum", *XXI-Ind Int. Symp. on Discharges and Electrical Insulation in vacuum-Matsue-2006*. pp. 140-143, DOI: 10.1109/DEIV.2006.357251
- [17] M.J. Barnes *et al.*, "Upgrade of the LHC injection kicker magnets", in *Proc. IPAC'13*, Shanghai, China, May 12-17 2013, paper MOPWA030, pp. 729-731. <http://www.JACoW.org>
- [18] M.J. Barnes *et al.*, "Operational experience of the upgraded LHC injection kicker magnets during Run 2 and future plans", *J. Phys. Conf. Ser.*, 874 (2017) 012101. <https://doi.org/10.1088/1742-6596/874/1/012101>
- [19] Polyteknik AS, DK-9750 Oestervraa, Denmark. <http://www.polyteknik.com/>
- [20] Heraeus Electronics, Heraeusstraße 12 - 14, 63450 Hanau, Germany, [www.heraeus-materials-technology.com](http://www.heraeus-materials-technology.com)
- [21] T. Baer *et al.*, "UFOs in the LHC: observations, studies and extrapolations", in *Proc. IPAC'12*, New Orleans, USA, May 21-26 2012, paper THPPP086, pp. 3936-3938. <http://www.JACoW.org>
- [22] B. Goddard *et al.*, "Transient beam losses in the LHC injection kickers from micron scale dust particles", in *Proc. IPAC'12*, New Orleans, USA, May 21-26 2012, TUPPR092, pp. 2044-2046. <http://www.JACoW.org>